Energy, Mines and Resources Canada
Énergie, Mines et Ressources Canada

CANMET

Canada Centre for Mineral and Energy Technology
Centre canadien de la technologie des minéraux et de l'énergie

Mining Research Laboratories
Laboratoires de recherche minière

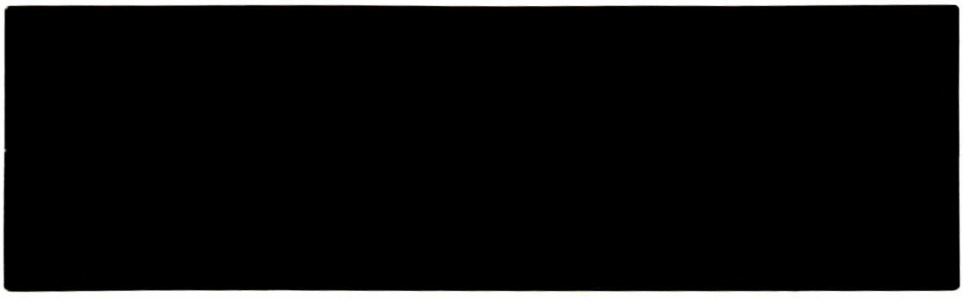

Canada

MRL 88-15(J) c.2

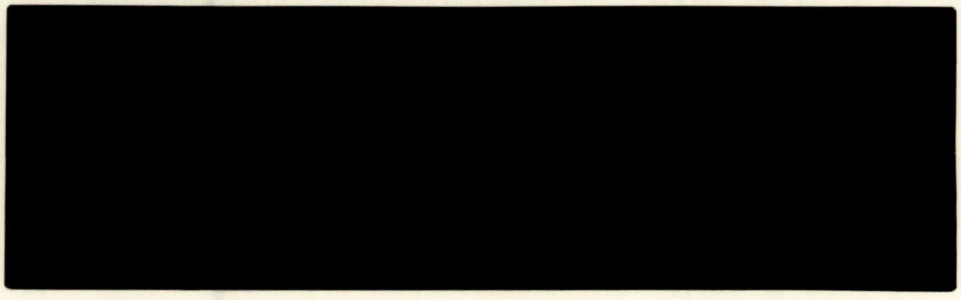

High Resolution Alpha-Particle-Spectrometry for Radium Analysis - the Effects of Sample Thickness and Filter Pore Size

TJOE-PA Lim, Nand K. DAVE and NORMAND R. CLOUTIER

ELLIOT LAKE LABORATORY

MRL 88-15 (J) c.2 CPUB

Published in Appl Radiat Isot Vol 40, No 1, pp 63-71, 1989
Int. J. Radiat Appl Instrum Part A
Printed in Great Britain

HRP 88-15(+)

Appl. Radiat. Isot. Vol. 40, No. 1, pp. 63–71, 1989
Int. J. Radiat. Appl. Instrum. Part A
Printed in Great Britain

0883-2889/89 $3.00 + 0.00
Pergamon Press plc

High Resolution Alpha-Particle-Spectrometry for Radium Analysis—the Effects of Sample Thickness and Filter Pore Size

TJOE-PA LIM, NAND K. DAVE* and NORMAND R. CLOUTIER

Elliot Lake Laboratory, CANMET, Energy, Mines and Resources Canada, P.O. Box 100. Elliot Lake, Ontario, Canada P5A 2J6

(*Received* 10 *February* 1987; *in revised form* 8 *April* 1988)

In the α-particle spectrometric technique for radium isotope analysis, the effects of the barium carrier thickness and pore size of the membrane filter (used for the main Ba–Ra sulphate filtration) on the resolution of the α-particle energy peaks were investigated. With 0.45 μm Millipore membrane filters, the full width at half maximum (FWHM) for 4.78 MeV α-decay peak of ^{226}Ra decreased from 221.7 to 121.3 keV with reduction in barium carrier additions from 320 to 20 μg Ba. The resolution further improved to 67.0 keV for 20 μg Ba carrier when 0.2 μm Nucleopore filters were used. There was also a significant decrease (20–50%) in the retention of radon and its daughters compared to their equilibrium concentrations as the barium carrier thickness was reduced.

A correlation study between ^{133}Ba tracer and ^{226}Ra isotopes recovery factors gave a recovery factor ^{226}Ra/^{133}Ba ratio of 0.93 ± 0.08 in the main Ba–Ra sulphate precipitate under various pH and sulphate concentration conditions.

Introduction

Radium isotopes are frequently monitored in environmental samples associated with the uranium industry. For α-emitting radionuclides such as ^{223}Ra, ^{224}Ra and ^{226}Ra, following a chemical separation of radium as Ba–Ra sulphates, an α-particle spectrometric technique using a silicon surface barrier detector provides a rapid method for the simultaneous measurement of their component fractions. There are, however, spectral-interference related problems in separating several parent and daugher radionuclide energy peaks when the overall system resolution is poor as reported in our previous study (Lim and Dave, 1981). During that study it was observed that the system resolution, defined as the full width at half maximum (FWHM) of the α-particle spectral line shape for a given energy peak, was low (FWHM ~229 keV) and depended on the amount of barium carrier added for co-precipitation, particle size of the final precipitate and its uniformity during deposition. Sill (1983) has also demonstrated the effects of these parameters and has shown that by reducing the crystal size of the final precipitate with the addition of a barium sulphate seeding suspension, a high α-resolution (FWHM 60 keV) with 97% analytical recovery can be obtained.

The amount of barium carrier added causes self-absorption and energy dispersion of α-particles, resulting in the broadening of the spectral line shapes. Theoretically, by decreasing the amount of the carrier added, the resolution of the α-particle energy spectrum can be improved, but the extent of improvement is limited by the required analytical recovery factors and is dependent upon the solubility of $BaSO_4$ in the final precipitating solution.

In the present study, we have investigated the effects of the deposited sample thickness in terms of barium carrier additions and the pore size of the membrane filter on:

(1) the overall resolution of the system:
(2) the analytical recovery factor: and
(3) the final equilibrium between Ra and its daughter products.

In a separate experiment we have further investigated the correlation between the recovery of ^{133}Ba tracer and ^{226}Ra isotopes in the final Ba–Ra sulphate precipitate over the entire range varying between 0 and 100% recovery which was obtained by altering various controlling parameters such as pH and sulphate concentration in the final precipitating solutions.

Method

The technique used here is a modification of our previous method described in detail by Lim and Dave

*Author for correspondence.

HIGH RESOLUTION ALPHA-SPECTROMETRY FOR RADIUM ANALYSIS THE EFFECTS OF SAMPLE THICKNESS AND FILTER PORE SIZE

(abbreviated title: HIGH RESOLUTION ALPHA-SPECTROMETRY)

Tjoe-Pa Lim, Nand K. Dave and Normand R. Cloutier
Elliot Lake Laboratory, CANMET, Energy, Mines and Resources Canada,
P.O. Box 100, Elliot Lake, Ontario, Canada, P5A 2J6

ABSTRACT

In the alpha-particle spectrometric technique for radium isotope analysis, the effects of the barium carrier thickness and pore size of the membrane filter (used for the main Ba-Ra sulphate filtration) on the resolution of the α-particle energy peaks were investigated. With 0.45 μm Millipore membrane filters, the full width at half maximum (FWHM) for 4.78 MeV alpha-decay peak of Ra-226 decreased from 221.7 keV to 121.3 keV with reduction in barium carrier additions from 320 μg to 20 μg Ba. The resolution further improved to 67.0 keV for 20 μg Ba carrier when 0.2 μm Nucleopore filters were used. There was also a significant decrease (20-50%) in the retention of radon and its daughters compared to their equilibrium concentrations as the barium carrier thickness was reduced.

A correlation study between Ba-133 tracer and Ra-226 isotopes recovery factors gave a recovery factor Ra-226/Ba-133 ratio of 0.93 $\pm$ 0.08 in the main Ba-Ra sulphate precipitate under various pH and sulphate concentration conditions.

(Address correspondence to N.K. Dave.)

INTRODUCTION

Radium isotopes are frequently monitored in environmental samples associated with the uranium industry. For α-emitting radionuclides such as Ra-223, Ra-224 and Ra-226, following a chemical separation of radium as Ba-Ra sulphates, an α-particle spectrometric technique using a silicon surface detector provides a rapid method for the simultaneous measurement of their component fractions. There are, however, spectral-interference related problems in separating several parent and daughter radionuclide energy peaks when the overall system resolution is poor as reported in our previous study (Lim, 1981). During that study it was observed that the system resolution, defined as the full width at half maximum (FWHM) of the α-particle spectral line shape for a given energy peak, was low (FWHM ~229 keV) and depended on the amount of barium carrier added for co-precipitation, particle size of the final precipitate and its uniformity during deposition. Sill (1983) has also demonstrated the effects of these parameters and has shown that by reducing the crystal size of the final precipitate with the addition of a barium sulphate seeding suspension, a high α-resolution (FWHM 60 keV) with 97% analytical recovery can be obtained.

The amount of barium carrier added causes self-absorption and energy dispersion of α-particles, resulting in the broadening of the spectral line shapes. Theoretically, by decreasing the amount of the carrier added, the resolution of the α-particle energy spectrum can be improved, but the extent of improvement is limited by the required analytical recovery factors and is dependent upon the solubility of $BaSo_4$ in the final precipitating solution.

In the present study, we have investigated the effects of the deposited sample thickness in terms of barium carrier additions and the pore size of the membrane filter on:

1) the overall resolution of the system;

2) the analytical recovery factor; and

3) the final equilibrium between Ra and its daughter products.

In a separate experiment we have further investigated the correlation between the recovery of Ba-133 tracer and Ra-226 isotopes in the final Ba-Ra sulphate precipitate over the entire range varying between 0 to 100% recovery which was obtained by altering various controlling parameters such as pH and sulphate concentration in the final precipitating solutions.

METHOD

The technique used here is a modification of our previous method described in detail by Lim et al. 1981, and Zimmerman et al. 1971, in which radium is separated chemically using barium as a carrier and co-precipitated as Ba-Ra sulphate. The method is a two-step separation, Ra is first co-precipitated along with sulphates of Pb and Ba added as carriers, the precipitate re-dissolved in ammoniacal solution of E.D.T.A. and finally precipitated as Ba-Ra sulphate at pH of 4.8. In order to obtain high resolution without greatly sacrificing the analytical recovery, a certain minimum amount of barium carrier concentration is required in the final precipitating solution. The minimum volume of the final solution is a critical parameter in controlling the thickness of the Ba-Ra sulphate deposition as the amount of barium carrier needed to exceed the solubility limit depends on the final volume. The method used here is based on a final volume of approximately 10 mL which contains 5 mL of 0.25 M ammoniacal E.D.T.A. (for complexing the primary precipitate containing Pb, Ba and Ra sulphates), 1 mL of saturated ammonium sulphate solution (100 g $(NH_4)_2$ SO_4/L) and 3 to 4 mL of glacial acetic acid.

For the self-absorption and high resolution study, eight samples were

prepared in duplicate, each containing 29.7 Bq of Ra-226 and a known amount (658.7 Bq) of Ba-133 tracer for recovery factor calculations. Varying amounts of barium carrier containing 320, 120, 90, 70, 50, 30, 25 and 20 μg of Ba were added to these samples. The samples were prepared according to the following modified procedure and deposited onto two types of membrane filters, Millipore 0.45 μm and Nucleopore 0.2 μm polycarbonate, to investigate the effect of filter pore size.

Following the primary precipitation procedure of Lim et al. (1981), the combined precipitate of Pb, Ba and Ra was filtered on a Millipore HABP 04700 (0.45 μm) filter. The filter paper was rolled with the deposited powder facing inside and transferred into a 25 mL test tube. The precipitate was dissolved in 5 mL of 0.25 M E.D.T.A. and three drops of concentrated ammonium hydroxide by heating the solution to near boiling. The filter paper was carefully removed from the test tube, counted for the residual Ba-133 activity and discarded if no residue was left. The solution was cooled, then 1 mL of saturated ammonium sulphate and 3 mL of glacial acetic acid were added, mixed well and allowed to stand for 15-20 min. The pH of the solution at this stage was ~4.8 and a faint cloudy precipitate of Ba-Ra sulphate appeared. The precipitate was filtered on Millipore HASP 02500 (0.45 μm) or Nucleopore 0.20 μm polycarbonate filters. After carefully rinsing the glass tube and filtering apparatus with 10% methanol, the filter paper was removed, glued onto an aluminum planchet with double sticky tape and dried in a desiccator. With this procedure the sample was prepared in less than an hour.

For Ba-Ra sulphate correlation study, forty samples were prepared in batches of 10 samples, each containing 270 mBq of Ra-226 and 658.7 Bq of Ba-133 tracer solution. The first batch of 10 samples was precipitated using the standard procedure described above. The next 20 samples were precipitated using the same procedure as above, but varying the pH of the final

precipitating solution between 3.9 and 6.5. The last batch of 10 samples was precipitated at pH 4.8, but having varying sulphate concentrations ranging from 0.05 to 125 mg of ammonium sulphate.

The Ra-226 standard solution for these studies was prepared using Amersham radium solution calibrated against an NBS standard and had an activity of 1188 $\pm$ 40 Bq/L. The Ba-133 tracer was prepared by diluting a stock solution to contain 65.87 Bq/mL of Ba-133 in the working solution. The samples were spiked with 10 mL of Ba-133 working solution.

The samples were counted for alpha and gamma activities using the experimental spectroscopy set-up described in detail by Lim et al. (1981). For α-particle energy spectra, the arrangement consisted of an Ortec ruggedized solid-state silicon surface barrier detector with 300 mm^2 surface area, a preamplifier, an amplifier and a bias voltage supply. The detector was positioned at approximately 2 mm from the source and measurements were performed under vacuum. A 4096 channel Canberra 40 pulse height analyzer was used for data acquisition. For γ-spectroscopy, a Harshaw Type 10.2 x 10.2 cm NaI(Tl) detector and a Tracor Northern data acquisition system was used.

RESULTS AND DISCUSSION

Figure 1 shows the observed α-particle spectra of Ra-226 obtained with barium carrier additions of 320 and 20 μg for 0.45 μm Millipore (a,b) and 20 μg barium for 0.2 μm Nucleopore polycarbonate (c) filters. The observed FWHM for 4.78 MeV decay peak for various carrier additions are given in Table 1. From these results, it can be seen that for 0.45 μm Millipore filters, the observed FWHM decreased from 221.7 keV for 320 μg barium to 121.3 keV for 20 μg barium carrier without any consistent trend as the carrier amount was decreased. The data showed a scattering trend for carrier amounts below 120 μg which was consistent for 0.45 μm Millipore filters. As pointed out in our

previous study by Lim (1981), and by Sill (1983) factors such as the uniformity of the deposited sample thickness and the particle size of the final precipitate became dominant below that range affecting the α-particle absorption characteristice and hence the overall resolution of the system. Sill (1983) improved the resolution to 60 KeV by reducing the crystal size of the final deposited precipitate with the addition of a barium sulphate seeding suspension to the final precipitating solution and also obtained high analytical recoveries (97%) for 100 μg Ba. Without the seeding suspension, his alpha resolutions of 130 to 270 KeV for 100 μg Ba using 0.1 μm Tuffryn filters are similar to our present results for 0.45 μm Millipore filters as the two procedures were basically similar.

In our study, we believed the resolution could be further improved by:

1. reducing the barium carrier concentration in the final precipitating solution to near its solubility limits, thereby decreasing the particle size of the precipitate: and
2. creating uniform depositional conditions by providing increased filter resistance. The latter was achieved by using 0.2 μm Nucleopore polycarbonate membrane filters which provided about three times higher resistance to liquid filtration than 0.45 μm Millipore filters as the variation in pore size distribution of the former was less.

Figure 1(c) shows the improvement in the resolution with 20 μg Ba where the FWHM decreased from 121.3 keV for 0.45 μm Millipore filters to between 67 to 74.5 keV for 0.2 μm Nucleopore filters. Similar values were obtained using Sill's (1983) method. The best resolutions obtained for commercially electro-deposited mixed radionuclides, Pu-239, Am-241 and Cm-244 source (Amersham) were respectively 70.3, 73.8 and 103.1 keV for 5.16 MeV Pu-239, 5.49 MeV Am-241 and 5.81 MeV Cm-244 α-particle energy peaks. A resolution of 67 keV was obtained for 5.49 MeV Rn-222 peak of a residual spectrum of Ra-226 daughters

attached to the detector surface after exposing the detector to a high activity (approximately 36 Bq) Ra-226 source for two hours. For the present sample detector geometry, the FWHM of the residual spectrum 67.0 keV represented the best achievable resolution of the system.

It is readily seen from these results that by depositing the final precipitate on 0.2 μm Nucleopore filters, the α-resolution of the system could be improved considerably to its practical limits without much loss in the analytical recovery factors ranging between 65 to 85% (Table 1). Because of the reduced Ba amounts these values are slightly lower than those of Sill's (1983). The advantage of the present method is that it is a simplified procedure requiring less preparation time.

The effect of the high resolution is clearly demonstrated in Figure 2 obtained for uranium tailings porewater samples containing Ra-223, Ra-224 and Ra-226 isotopes. For comparison purposes, Figure 2(c) also shows a Ra-226 spectrum obtained with a 0.2 μm Nucleopore filter and 20 μg barium carrier. Note the resolution of 4.602 MeV (5.55%), and 4.785 MeV Ra-226 peaks, similar to those described by Sill (1983).

From Figure 2 it is evident that although there is a clear separation of Ra-226 peaks from those of Ra-223 and Ra-224, component resolutions among Rn-222 (5.490 MeV), Ra-223 (5.61, 5.71 and 5.75 MeV), and Ra-224 (5.45 and 5.68 MeV) peaks is not possible because of spectral interference. Thus, in a sample containing all three isotopes, Ra-226 can be measured directly, but the presence of the other two isotopes can only be inferred qualitatively. Indirect determinations of Ra-223 and Ra-224 from their daughter products (Po-215 for Ra-223), and (Po-212 for Ra-224) which are clearly resolved (as shown in Figure 2) can be accomplished after a certain ingrowth period provided appropriate corrections are made for the loss of radon isotopes from the sample. Table 2 shows the equilibrium ratios for Rn-222/Ra-226, and Po-218/

Rn-222 for Ra-222, and Po-214/Rn-222 for Ra-226 isotope after an ingrowth period of 60 days.

It can be seen here that with the decrease in the barium carrier concentration, there is a significant loss of radon gas from the sample with only 55% of the equilibrium concentration retained for a sample containing 20 μg Ba carrier. The loss of radon gas is caused by the decrease in the diffusion path related to crystal size and attenuation of the recoil radon atoms as the carrier thickness is reduced. On the other hand, the equilibrium ratio between radon and its daughter products is close to 95% for all samples having resolution between 67 to 120 keV, and Ba carrier 20 to 40 μg. For samples containing a higher concentration of barium carrier (320 μg, FWHM = 221.7 keV), the calculated ratio between radon and daughter products is less than 100% which was caused by the poor resolution of Ra-226, Ra-222 and Po-218 peaks as the spectral overlap was significant (see Figure 1).

For a given sample, the measured retention ratio for Rn-222/Ra-226 at equilibrium can be used to correct for daughter activities in calculating Ra-223 and Ra-224 from their ingrown daughter concentrations. Alternatively, in a sample containing Ra-223 and Ra-224 isotopes, their activities can also be determined as follows:

1. At the time $t=t_o$ ($\sim$0), immediately following the separation of radium isotopes from their parents, determine the combined activity, X, of Ra-223 and Ra-224 from their integrated decay peaks (5.45 to 5.71 MeV), such that:

$$A\ C_{Ra\text{-}223}(0) + B\ C_{Ra\text{-}224}(0) = X\ (Bq)\ \text{at}\ t=t_o \qquad \text{Eq 1}$$

where, A = activity fraction of Ra-223 at $t=t_o = e^{-\lambda_1 t_o}$

B = activity fraction of Ra-224 at $t=t_o = e^{-\lambda_1' t_o}$

$C_{Ra\text{-}223}(0)$ = activity of Ra-223 at t=0

$C_{Ra\text{-}224}(0)$ = activity of Ra-224 at t=0, and

λ_1, and λ_1' are decay constants for Ra-223 and Ra-224, respectively.

It is assumed in the above expression that the activity of ingrown Rn-222 daughters from the Ra-226 isotope was negligibly small for the short counting period.

2. After a certain ingrowth period of daughters, at time $t=t_g$, determine the activity ratio of Po-215/Po-212 as:

$$\frac{\text{Po-215 } (t_g)}{\text{Po-212 } (t_g)} = Y \qquad \text{Eq 2}$$

where, the activities of Po-215 and Po-212 at $t=t_g$ are given by:

$$\text{Po-215}(t_g) = D\ C_{\text{Ra-223}}(0)$$

$$\text{Po-212}(t_g) = F\ C_{\text{Ra-224}}(0) \qquad \text{Eq 3}$$

where, D and F are expressed in terms of decay constants as:

$$D = \frac{\lambda_{\text{Po-215}}}{\lambda_{\text{Ra-223}}} \left(\sum_{n=1}^{3} a_{3n}\ e^{-\lambda_n t_g}\right) \qquad \text{Eq 4}$$

for Ra-223 series, and

$$F = \frac{\lambda'_{\text{Po-212}}}{\lambda'_{\text{Ra-224}}} .Br. \left(\sum_{n=1}^{6} a_{6n}\ e^{-\lambda' n t_g}\right) \qquad \text{Eq 5}$$

for Ra-224 series,

where, Br = branching ratio (0.64) for Bi-212 to Po-212, and

$$a_{mn} = \frac{\lambda_1\ \lambda_2 \ldots \lambda_{m-1}}{(\lambda_m-\lambda_n)(\lambda_{m-1}-\lambda_n)\ldots(\lambda_{m-r}-\lambda_n)(\lambda_2-\lambda_n)(\lambda_1-\lambda_n)} \qquad \text{Eq 6}$$

where, $m>n$ and $m-r \neq n$.

$$a_{mm} = \frac{\lambda_1\ \lambda_2 \ldots \lambda_{m-1}}{(\lambda_{m-1}-\lambda_m)(\lambda_{m-2}-\lambda_m)\ldots(\lambda_1-\lambda_m)} \qquad \text{Eq 7}$$

for $m = n$.

$\lambda_1, \lambda_2 \ldots \lambda_n$ = decay constants of Ra-223, Rn-219 and Po-215, etc.

$\lambda'_1 \ldots \lambda'_n$ = decay constants of Ra-224, Rn-220...Po-212, etc.

Solving Equations 1 to 3 we have:

$$C_{\text{Ra-223}}(0) = \frac{X\ Y\ F}{(AYF + BD)} \qquad \text{Eq 8}$$

and,

$$C_{\text{Ra-224}}(0) = \frac{X\ D}{(AYF + BD)} \qquad \text{Eq 9}$$

Thus, the concentrations of Ra-223 and Ra-224 can be obtained by measuring parameters X and Y with A, B, D and F.

It was assumed in the above derivations that there was no significant difference in the retention characteristics of various radon isotopes and their daughter products for the three radium isotopes. Use of computerized models such as those developed by Wätzig, et al. (1978), Westmeier (1984), and Williams (1984) for complex α-particle spectra could further the analytical capabilities of the present high resolution technique.

BARIUM-RADIUM RECOVERY

Table 3 gives the calculated recovery factors for Ba-133 and Ra-226. true and corrected Ra-226 counts at 100% recovery for 6000 sec. The recovery factors for Ra-226 were calculated using the measured value of the instrumental efficiency factor, ε = 0.224 and source disintegration per minute (dpm) = 22.2, equivalent to total counts per 6000 sec = 497. The observed frequency distributions for Ba-133 and Ra-226 recovery factors are plotted in Figure 3. Figure 4 shows the correlation between the observed Ra-226 counts and Ba-133 recovery factors with a linear relationship of the form:

Y (Ra-226 counts/6000 sec) = 4.57 . (% Ba-133 recovery)

with the coefficient of regression r^2 = 0.98 and standard deviation of the slope = 0.05.

Also shown in Table 3 and Figure 4, are the observed and calculated Ra-226 counts at 100% recovery (curve 'D'). Note that the average Ra-226 counts calculated for 100% recovery were 465 $\pm$ 44 compared to the expected value of 497, the difference being of no statistical significance ($p > 0.05$). Figure 5 shows the correlation between the two calculated recovery factors for Ra-226 and Ba-133. The average value of the Ra-226/Ba-133 recovery ratio was calculated as 0.93 $\pm$ 0.08 compared to the expected value of 1.0. In the final

$BaSO_4$ precipitation procedure, it was aimed at varying the overall recovery of Ba and Ra sulphates over a wide range by adjusting the controlling parameters such as pH and sulphate concentrations, but the final recovery was always high (>60%) except for eight samples where it was zero and for two samples where it varied from 10 to 30%. No attempt was made to vary the barium carrier concentration to obtain different recovery factors as such was not the case in the routine analytical procedure where the carrier concentration was always constant. As seen from the data no systematic trends between low and high recoveries were identifiable.

It can thus be stated from present results that by using a chemically different isotope as a tracer (Ba-133) to measure chemical yield of Ra isotopes, the correlation between the two can only be expressed within a statistical uncertainty of approximately 8%. As Sill (1983) has pointed out, better correlation between these two atoms differing in ionic radii and chemical characteristics cannot be expected to the same degree as in the case with similar isotopic tracers. For Ra-226 analysis, however, there are no other radium isotopes with reasonable half-lives that can be used as tracers.

CONCLUSIONS

This study has clearly demonstrated that the α-particle resolution of the system can be improved by a factor of 3 by decreasing the barium carrier concentration to 20 μg and using a 0.2 μm Nucleopore membrane filter, without much loss in chemical recovery. The overall effect was to reduce the broadening of the α-spectral peaks because of self-absorption of α-particles within the deposited barium sulphate and its crystalline matrix. There was also a significant decrease in the retention of radon and its daughters with the decrease of barium carrier.

Correlation between Ba-133 and Ra-226 isotopic recovery factors showed

that for the main Ba-Ra sulphate precipitates, the recovery factors between these two chemically different atoms can only be expressed within a statistical uncertainty of ±8%.

REFERENCES

Lim, T.P. and Dave, N.K., (1981) "A rapid method of Ra-226 analysis in water samples using an alpha-spectroscopic technique"; CIM Bull. vol 74, No. 833, p. 97.

Sill, C.W., (1983) "Determination of radium-226 by high resolution alpha-spectrometry"; Report DE83-014 959, EG&G Inc., Idaho Falls, Idaho, U.S.A.;

Wätzig, W. and Westmeier, W., (1978) "Alfun - a program for the evaluation of complex alpha-spectra"; Nuclear Instrum & Methods, vol. 153, p. 517.

Westmeier, W., (1984) "Computerized analysis of alpha-particle spectra"; Int J Appl Rad & Isotopes, vol. 35, No. 4, pp. 263-270.

Williams, R.L., (1984) "A computerized alpha-particle-spectrometry system for the analysis of low-level thorium, uranium, plutonium and americium fractions"; Int J Appl Rad & Isotopes, vol. 35, No. 4, pp. 271-277.

Zimmerman, J.B. and Armstrong, V.C., (1971) "The determination of Ra-226 in uranium ores and mill products by alpha-energy spectra"; Division Report MRP/MRL 76-11, CANMET, Energy, Mines and Resouces Canada.

TABLE CAPTIONS

1. Full width half maximum (FWHM) for Ra-226, 4.75 MeV peak for various amounts of barium carrier added. The area of the source was 1.815 cm^2 and detector source spacing $\sim$0.2 cm.

2. Equilibrium ratio between Ra-226 and its daughter isotopes: Ra-222, Po-218 and Po-214 at time t = 60 days after radium separation. Expected equilibrium ratio = 100%.

3. Comparisons between Ba-133 and Ra-226 recovery factors and the observed (true) and Ra-226 counts at 100% recovery. Ra-226 recovery factors were calculated using the instrumental efficiency factor ε = 0.224, and true counts = 497.5.

Table 1 - Full width half maximum (FWHM) for Ra-226, 4.78 MeV peak for various amounts of barium carried added. The area of the source was 1.815 cm^2 and source detector spacing ~0.2 cm.

Barium Carrier Added μg	Recovery Factor Ba-133 %	Calc. Barium Carrier Thickness $\mu g/cm^2$ (for uniform depisition)	FWHM KeV
	Filter type: Millipore, 0.45 μm HABP 02500		
320	91.3	161.0	221.7
120	56.3	37.2	188.5
90	91.8	45.5	116.2
70	89.4	34.5	168.2
50	98.0	27.0	134.3
30	74.5	12.3	166.0
25	79.8	11.0	127.8
20	84.6	9.3	121.3
250	81.0	111.6	229*
100	67.5	37.2	229*
	Filter type: Nucleopore, 0.2 μm polycarbonate		
20	67.4	7.4	74.5
20	65.6	7.2	67.0

* Data from Lim et al. (1981).

Table 2 - Equilibrium ratio between Ra-226 and its daughter isotopes: Ra-222, Po-218 and Po-214 at time t = 60 days after radium separation. Expected equilibrium ratio = 100%.

Sample No.	FWHM (keV)	Rn-222/Rn-226 (%)	Po-218/Rn-222 (%)	Po-214/Rn-222 (%)	
1	221.7	106.1	77.1	84.7	
2	120.0	84.0	100.0	96.4	
3	76.0	72.0	93.1	95.9	$\bar{X}$=94.8
4	67.0	55.0	92.7	90.8	σ=3.3

Note: Sample 1 - Ra-226 standard solution precipitate deposited on 0.45 μm Millipore filter; barium carrier = 320 μg.

Sample 2 - Ra-226 standard solution precipitate deposited on 0.22 μm Millipore filter; barium carrier = 40 μg.

Sample 3 - Ra-226 standard solution precipitate deposited on 0.2 μm Nucleopore polycarbonate filter; barium carrier = 40 μg

Sample 4 - Ra-226 standard solution precipitate deposited on 0.2 μm Nucleopore polycarbonate filter; barium carrier = 20 μg.

Table 3 - Comparisons between Ba-133 and Ra-226 recovery factors and the observed (true) and Ra-226 counts at 100% recovery. Ra-226 recovery factors were calculated using the instrumental efficiency factor ε=0.224, and true counts = 497.5.

Sample No.	Remark	Recovery Ba-133 %	Ra-226 Counts/ 6000 s	100% Ra-226 Counts/ 6000 s	Recovery Ra-226 %	Recovery Ratio %Ra/%Ba
1	Std. procedure	71.6	382	534	76.8	1.07
2	Std. procedure	90.4	454	502	91.3	1.01
3	Std. procedure	90.4	408	451	82.0	0.91
4	Std. procedure	90.5	400	442	80.4	0.89
5	Std. procedure	87.8	393	447	79.0	0.90
6	Std. procedure	86.8	406	468	81.6	0.94
7	Std. procedure	87.0	391	450	78.6	0.90
8	Std. procedure	85.0	371	436	74.6	0.88
9	Std. procedure	90.0	413	459	83.0	0.92
10	Std. procedure	86.7	384	443	77.2	0.89
11	Prec. at pH=5.90*	76.2	369	484	74.2	0.97
12	Prec. at pH=5.45	81.0	404	499	81.2	1.00
13	Prec. at pH=4.98	92.4	420	455	84.5	0.91
14	Prec. at pH=4.48	88.7	347	391	69.8	0.79
15	Prec. at pH=3.95	97.6	385	395	77.4	0.79
16	Prec. at pH=5.98	89.8	390	434	78.4	0.87
17	Prec. at pH=5.25	87.9	389	443	78.2	0.89
18	Prec. at pH=4.99	99.3	462	465	92.9	0.94
19	Prec. at pH=5.30	97.5	416	427	83.7	0.86
20	Prec. at pH=4.56	68.8	329	478	66.2	0.96
21	Prec. at pH=4.68	24.4	98	402	19.7	0.81
22	pH=1.18; pH=5.5**	77.0	374	486	75.2	0.98
23	pH=3.42; pH=6.5	0.0	6	465	1.2	-
24	pH=3.38; pH=6.0	0.0	2	465	0.4	-
25	pH=3.3; pH=5.5	67.3	312	464	62.7	0.93
26	pH=3.25; pH=5.25	83.1	376	452	75.6	0.91
27	pH=3.3; pH=5.0	79.4	350	441	70.4	0.89
28	pH=3.4; pH-4.8	68.2	331	485	66.6	0.98
29	pH=3.0; pH=6.5	0.0	2	465	0.4	-
30	pH=3.42; pH=4.8	80.0	331	414	66.6	0.83
31	Final+0.05mg AS+	0.0	2	465	0.4	-
32	Final+50mg "	0.0	2	465	0.4	-
33	Final+21mg "	0.0	1	465	0.2	-
34	Final+125mg "	13.7	80	583	16.1	1.17
35	Final+115mg "	72.2	373	517	75.0	1.04
36	Final+75mg "	56.3	292	519	58.7	1.04
37	Final+2mg "	0.0	3	465	0.6	-
38	Final+50mg "	0.0	2	465	0.4	-
39	Final+75mg "	67.0	341	509	68.6	1.02
40	Final+100mg "	74.0	371	501	74.6	1.01
			Average:	464.9		0.93
			Std. Dev:	44		0.08

* Final precipitation at specified pH.
** First precipitation at pH = 1.18, and second at pH = 5.5
\+ AS - Amount of ammonium sulphate added to final precipitating solution

FIGURE CAPTIONS

Figure 1 - Ra-226 alpha-particle energy spectra using 0.45 μm Millipore filter with barium carrier (a) 320 μg; (b) 20 μg; and (c) 0.20 μm Nucleopore polycarbonate filter with 20 μg Ba. FWHM = full width at half measure.

Figure 2 - Expanded alpha-particle energy spectra of radium isotopes (a) 0.45 μm Millipore with 320 μg Ba; (b) 0.20 μm Nucleopore with 40 μg Ba; and (c) Ra-226 spectrum only, 0.2 μm Nucleopore with 20 μg Ba.

Figure 3 - Frequency distribution of Ba-113 and Ra-226 recovery factors.

Figure 4 - Correlation between the observed Ra-226 counts and Ba-133 recovery factor curve (A) and with 95% confidence limits (curves B and C). Curve D is the calculated Ra-226 counts at 100% efficiency.

Figure 5 - Correlation between the actual Ra-226 and Ba-133 recovery factors (curve A), 95% confidence limits (curves B and C).

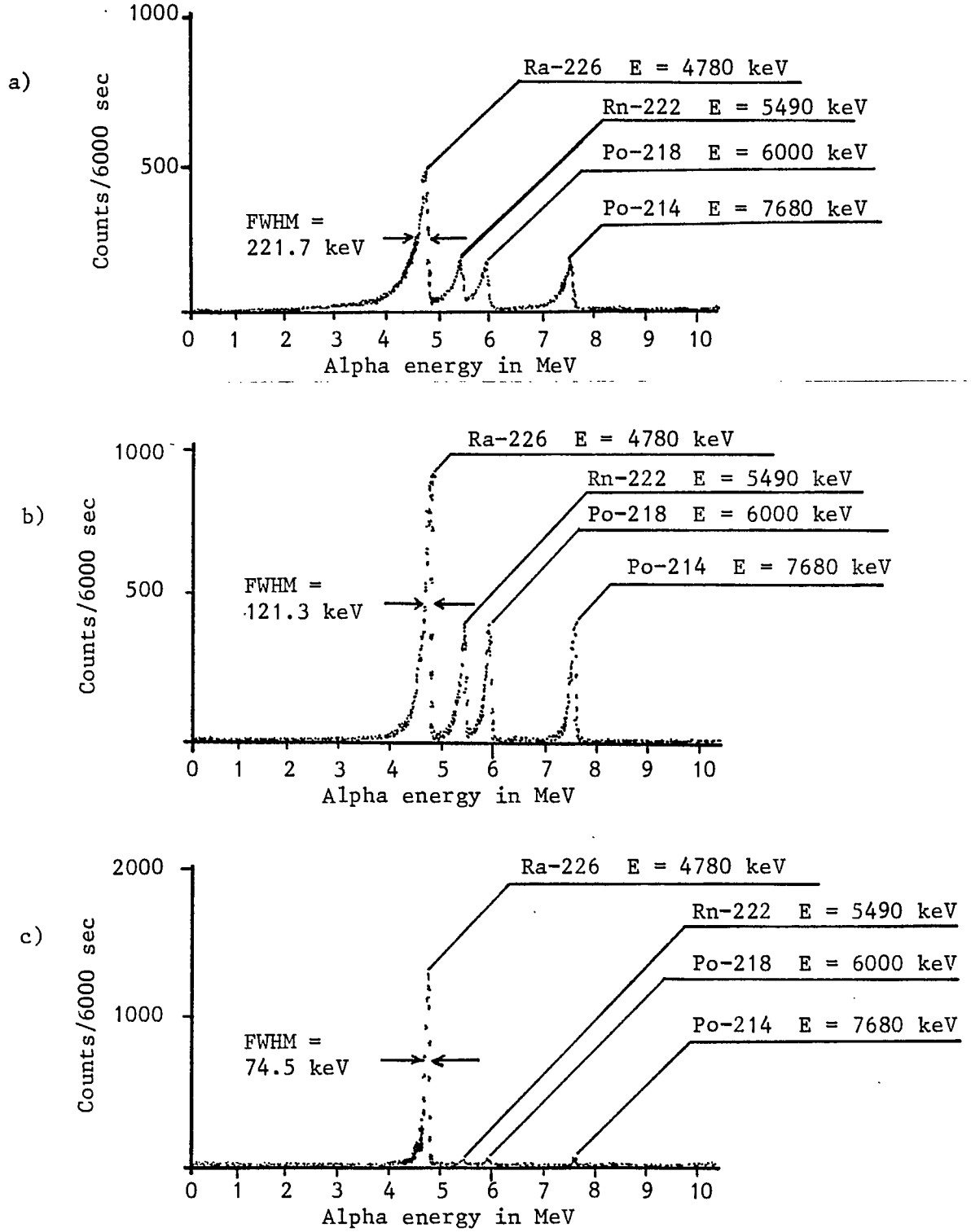

Fig. 1 - Ra-226 alpha-particle energy spectra using: 0.45 μm Millipore filter with barium carrier: a) 320 μg; b) 20 μg; and c) 0.20 μm Nucleopore polycarbonate filter with 20 μg Ba. FWHM = full width at half maximum.

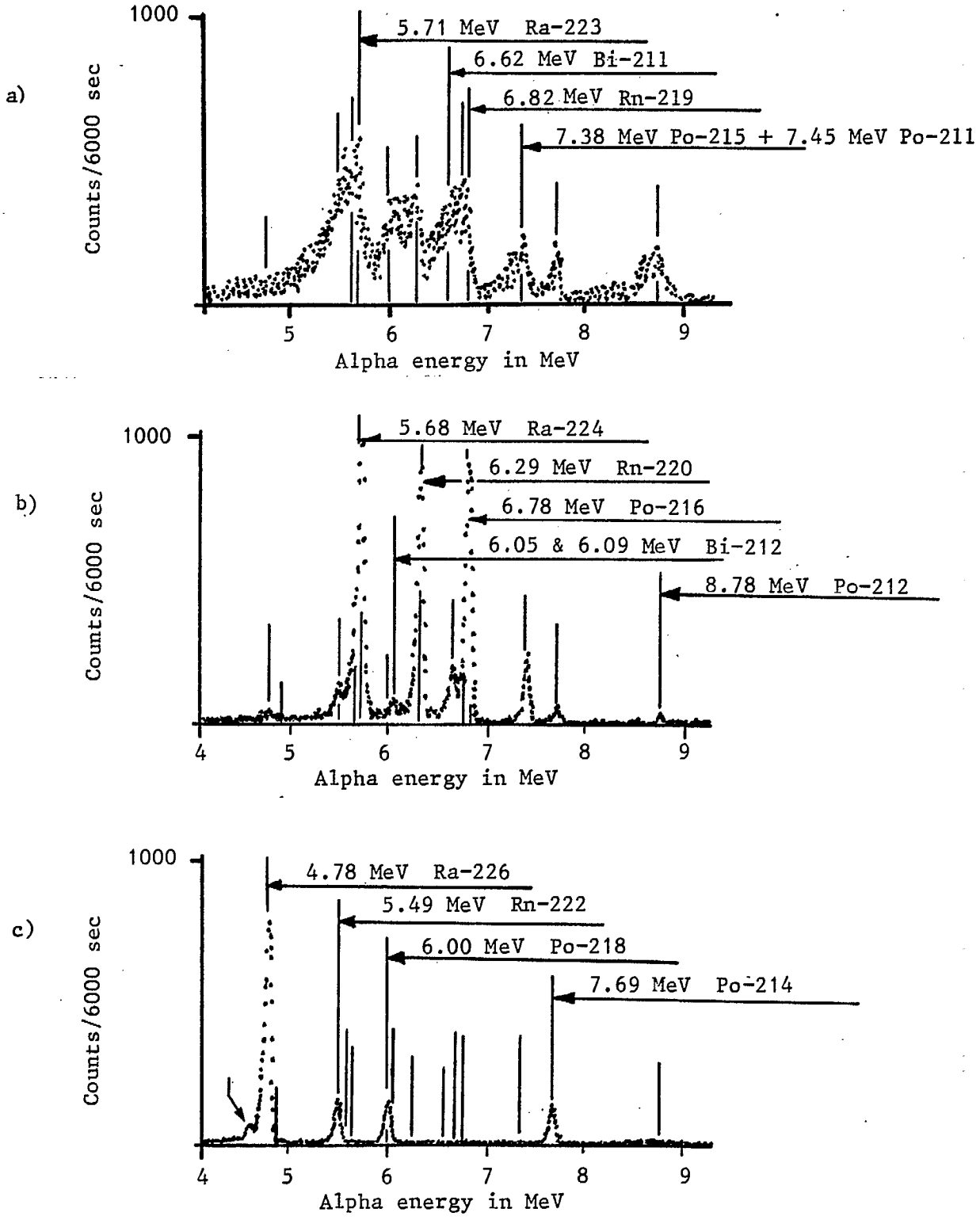

Fig. 2 - Expanded alpha-particle spectra of radium isotopes: a) 0.45 μm Millipore with 320 μg Ba; b) 0.20 μm Nucleopore with 40 μg Ba; and c) Ra-226 spectrum only, 0.20 μm Nucleopore with 20 μg Ba.

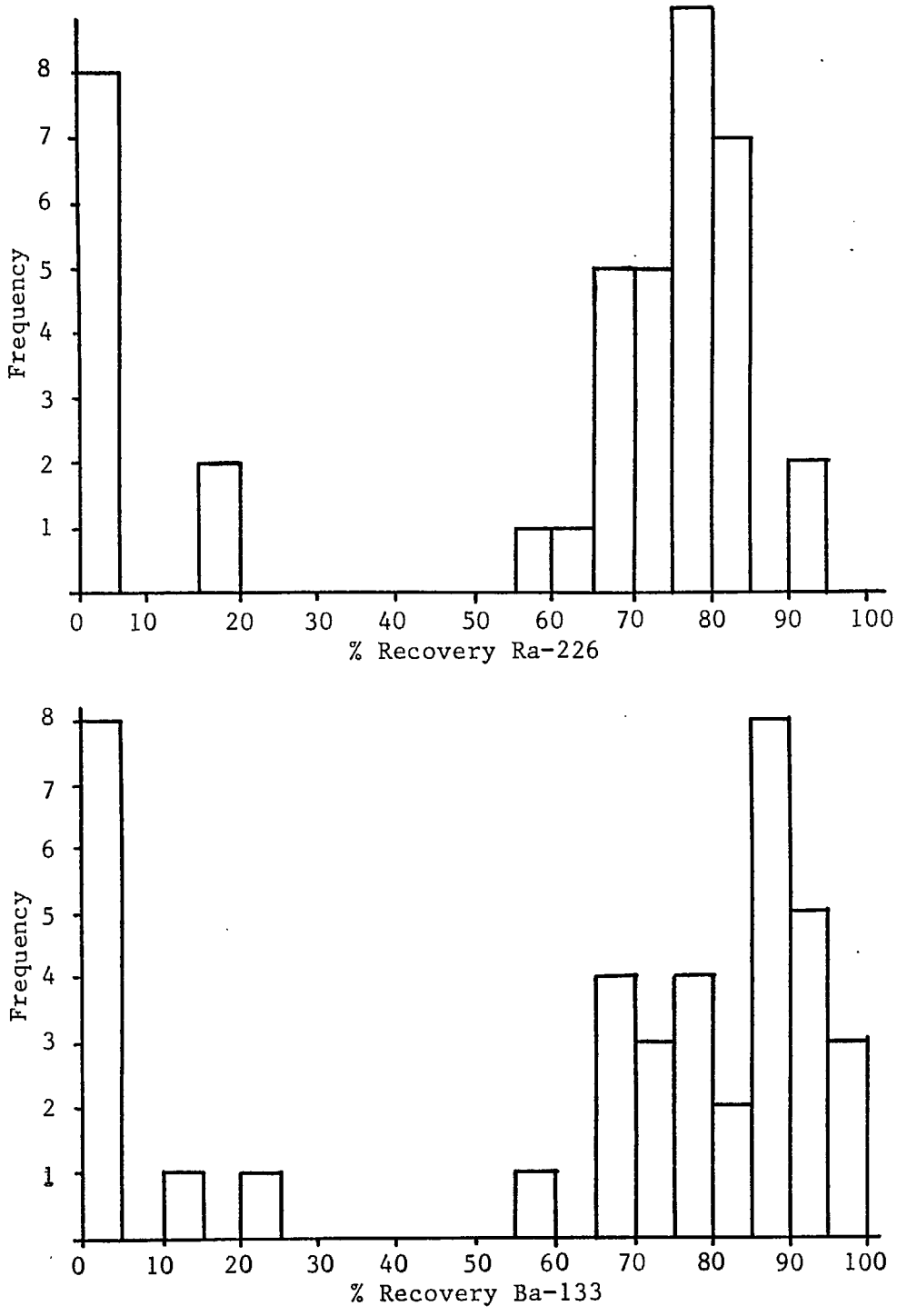

Fig. 3 - Frequency distribution of Ba-133 and Ra-226 recovery factors.

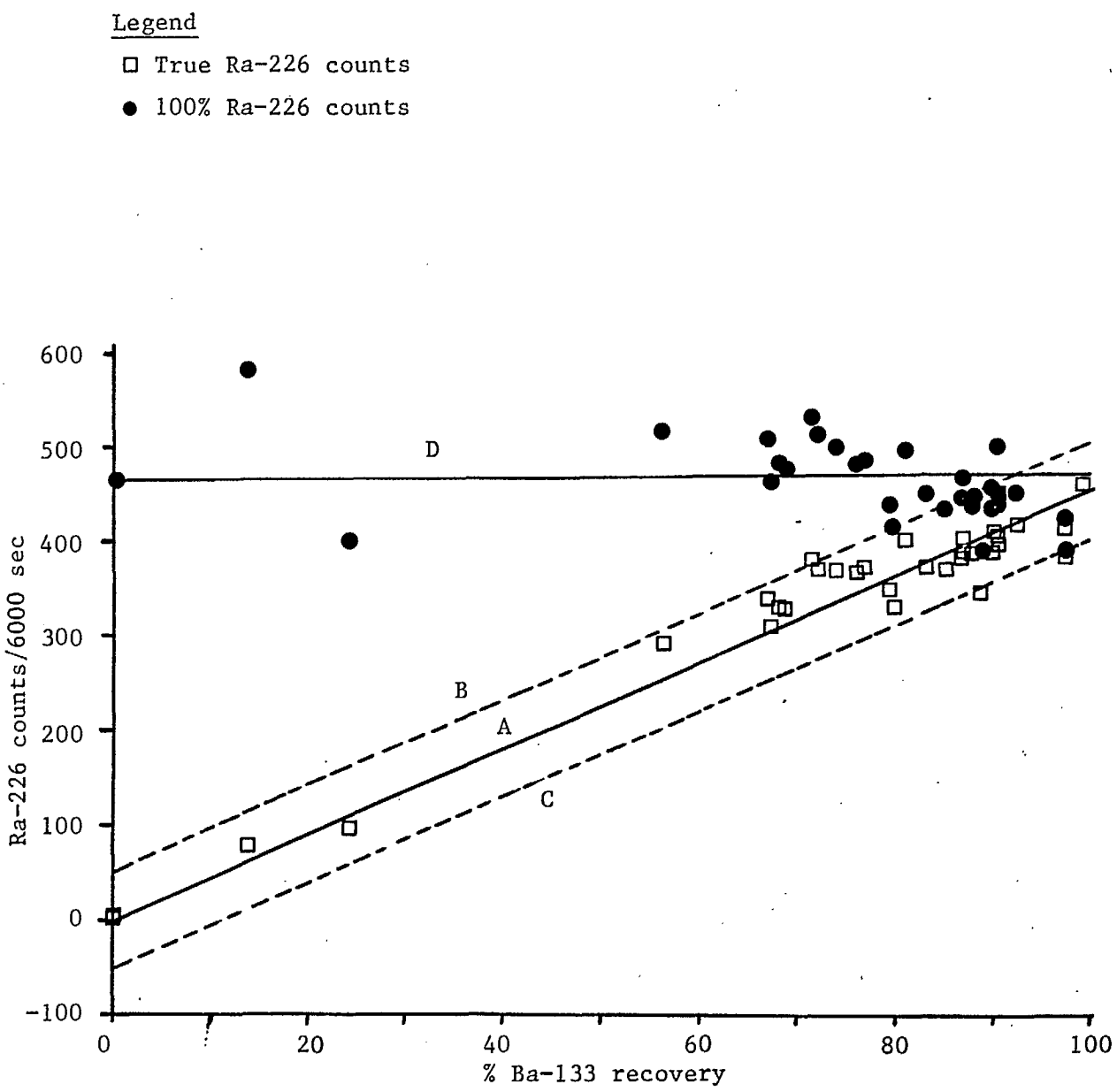

Fig. 4 - Correlation between the observed Ra-226 counts and Ba-133 recovery factor curve (A) with 95% confidence limits (curves B and C). Curve D is the calculated Ra-226 counts at 100% efficiency.

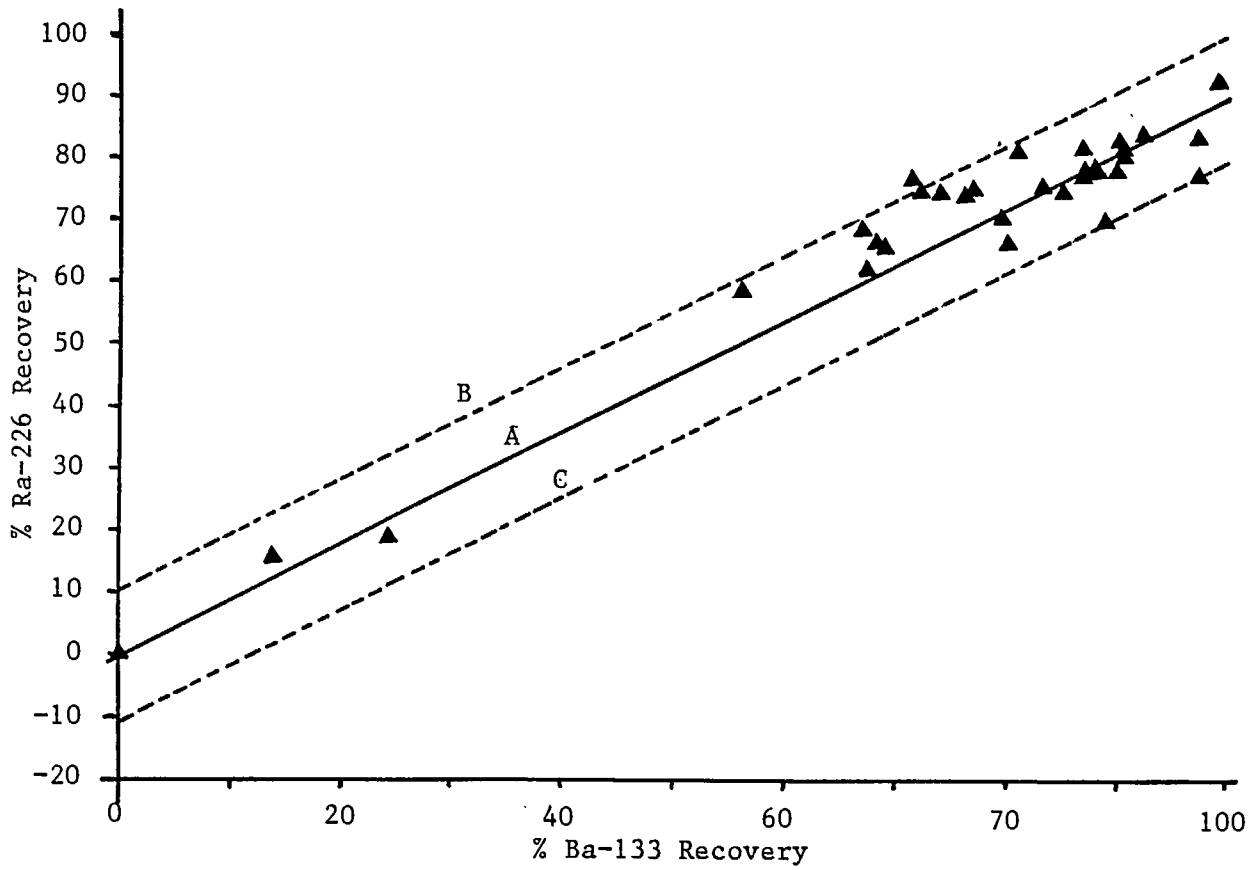

Fig. 5 - Correlation between the actual Ra-226 and Ba-133 recovery factors (curve A), 95% confidence limits (curves B and C).

Appl. Radiat. Isot. Vol. 40, No. 1, pp. 63–71, 1989
Int. J. Radiat. Appl. Instrum. Part A
Printed in Great Britain

0883-2889/89 $3.00 + 0.00
Pergamon Press plc

High Resolution Alpha-Particle-Spectrometry for Radium Analysis—the Effects of Sample Thickness and Filter Pore Size

TJOE-PA LIM, NAND K. DAVE* and NORMAND R. CLOUTIER

Elliot Lake Laboratory, CANMET, Energy, Mines and Resources Canada, P.O. Box 100. Elliot Lake, Ontario, Canada P5A 2J6

(*Received* 10 *February* 1987; *in revised form* 8 *April* 1988)

In the α-particle spectrometric technique for radium isotope analysis, the effects of the barium carrier thickness and pore size of the membrane filter (used for the main Ba–Ra sulphate filtration) on the resolution of the α-particle energy peaks were investigated. With 0.45 μm Millipore membrane filters, the full width at half maximum (FWHM) for 4.78 MeV α-decay peak of ^{226}Ra decreased from 221.7 to 121.3 keV with reduction in barium carrier additions from 320 to 20 μg Ba. The resolution further improved to 67.0 keV for 20 μg Ba carrier when 0.2 μm Nucleopore filters were used. There was also a significant decrease (20–50%) in the retention of radon and its daughters compared to their equilibrium concentrations as the barium carrier thickness was reduced.

A correlation study between ^{133}Ba tracer and ^{226}Ra isotopes recovery factors gave a recovery factor ^{226}Ra/^{133}Ba ratio of 0.93 ± 0.08 in the main Ba–Ra sulphate precipitate under various pH and sulphate concentration conditions.

Introduction

Radium isotopes are frequently monitored in environmental samples associated with the uranium industry. For α-emitting radionuclides such as ^{223}Ra, ^{224}Ra and ^{226}Ra, following a chemical separation of radium as Ba–Ra sulphates, an α-particle spectrometric technique using a silicon surface barrier detector provides a rapid method for the simultaneous measurement of their component fractions. There are, however, spectral-interference related problems in separating several parent and daugher radionuclide energy peaks when the overall system resolution is poor as reported in our previous study (Lim and Dave, 1981). During that study it was observed that the system resolution, defined as the full width at half maximum (FWHM) of the α-particle spectral line shape for a given energy peak, was low (FWHM ~229 keV) and depended on the amount of barium carrier added for co-precipitation, particle size of the final precipitate and its uniformity during deposition. Sill (1983) has also demonstrated the effects of these parameters and has shown that by reducing the crystal size of the final precipitate with the addition of a barium sulphate seeding suspension, a high α-resolution (FWHM 60 keV) with 97% analytical recovery can be obtained.

The amount of barium carrier added causes self-absorption and energy dispersion of α-particles, resulting in the broadening of the spectral line shapes. Theoretically, by decreasing the amount of the carrier added, the resolution of the α-particle energy spectrum can be improved, but the extent of improvement is limited by the required analytical recovery factors and is dependent upon the solubility of $BaSO_4$ in the final precipitating solution.

In the present study, we have investigated the effects of the deposited sample thickness in terms of barium carrier additions and the pore size of the membrane filter on:

(1) the overall resolution of the system:
(2) the analytical recovery factor: and
(3) the final equilibrium between Ra and its daughter products.

In a separate experiment we have further investigated the correlation between the recovery of ^{133}Ba tracer and ^{226}Ra isotopes in the final Ba–Ra sulphate precipitate over the entire range varying between 0 and 100% recovery which was obtained by altering various controlling parameters such as pH and sulphate concentration in the final precipitating solutions.

Method

The technique used here is a modification of our previous method described in detail by Lim and Dave

*Author for correspondence.

(1981), and Zimmerman *et al.* (1971), in which radium is separated chemically using barium as a carrier and co-precipitated as Ba–Ra sulphate. The method is a two-step separation, Ra is first co-precipitated along with sulphates of Pb and Ba added as carriers, the precipitate re-dissolved in ammoniacal solution of EDTA and finally precipitated as Ba–Ra sulphate at pH of 4.8. In order to obtain high resolution without greatly sacrificing the analytical recovery, a certain minimum amount of barium carrier concentration is required in the final precipitating solution. The minimum volume of the final solution is a critical parameter in controlling the thickness of the Ba–Ra sulphate deposition as the amount of barium carrier needed to exceed the solubility limit depends on the final volume. The method used here is based on a final volume of approximately 10 mL which contains 5 mL of 0.25 M ammonical EDTA (for complexing the primary precipitate containing Pb, Ba and Ra sulphates), 1 mL of saturated ammonium sulphate solution (100 g $(NH_4)_2SO_4$/L) and 3–4 mL of glacial acetic acid.

For the self-absorption and high resolution study, eight samples were prepared in duplicate, each containing 29.7 Bq of ^{226}Ra and a known amount of (658.7 Bq) of ^{133}Ba tracer for recovery factor calculations. Varying amounts of barium carrier containing 320, 120, 90, 70, 50, 30, 25 and 20 μg of Ba were added to these samples. The samples were prepared according to the following modified procedure and deposited onto two types of membrane filters: Millipore 0.45 μm and Nucleopore 0.2 μm polycarbonate, to investigate the effect of filter pore size.

Following the primary precipitation procedure of Lim and Dave (1981), the combined precipitate of Pb, Ba and Ra was filtered on a Millipore HABP 04700 (0.45 μm) filter. The filter paper was rolled with the deposited powder facing inside and transferred into a 25 mL test tube. The precipitate was dissolved in 5 mL of 0.25 M EDTA and three drops of concentrated ammonium hydroxide by heating the solution to near boiling. The filter paper was carefully removed from the test tube, counted for the residual ^{133}Ba activity and discarded if no residue was left. The solution was cooled, then 1 mL of saturated ammonium sulphate and 3 mL of glacial acetic acid were added, mixed well and allowed to stand for 15–20 min. The pH of the solution at this stage was ~4.8 and a faint cloudy precipitate of Ba–Ra sulphate appeared. The precipitate was filtered on Millipore HASP 02500 (0.45 μm) or Nucleopore 0.20 μm polycarbonate filters. After carefully rinsing the glass tube and filtering apparatus with 10% methanol, the filter paper was removed, glued onto an aluminium planchet with double sticky tape and dried in a desiccator. With this procedure the sample was prepared in less than 1 h.

For the Ba–Ra sulphate correlation study, 40 samples were prepared in batches of 10 samples, each containing 270 mBq of ^{226}Ra and 658.7 Bq of ^{133}Ba tracer solution. The first batch of 10 samples was precipitated using the standard procedure described above. The next 20 samples were precipitated using the same procedure as above, but varying the pH of the final precipitating solution between 3.9 and 6.5. The last batch of 10 samples was precipitated at pH 4.8, but having varying sulphate concentrations ranging from 0.05 to 125 mg of ammonium sulphate.

The ^{226}Ra standard solution for these studies was prepared using Amersham radium solution calibrated against an NBS standard and had an activity of 1188 ± 40 Bq/L. The ^{133}Ba tracer was prepared by diluting a stock solution to contain 65.87 Bq/mL of ^{133}Ba in the working solution. The samples were spiked with 10 mL of ^{133}Ba working solution.

The samples were counted for α and γ activities using the exprimental spectroscopy set-up described in detail by Lim and Dave (1981). For α-particle energy spectra, the arrangement consisted of an Ortec ruggedized solid-state silicon surface barrier detector with 300 mm^2 surface area, a preamplifier, an amplifier and a bias voltage supply. The detector was positioned at approx 2 mm from the source and measurements were performed under vacuum. A 4096 channel Canberra pulse height analyzer was used for data acquisition. For γ-spectroscopy, a Harshaw 10.2×10.2 cm NaI(Tl) detector and a Tracor Northern data acquistion system was used.

Results and Discussion

Figure 1 shows the observed α-particle spectra of ^{226}Ra obtained with barium carrier additions of 320 and 20 μg for 0.45 μm Millipore (a, b) and 20 μg barium for 0.2 μm Nucleopore polycarbonate (c) filters. The observed FWHM for the 4.78 MeV decay peak for various carrier additions are given in Table 1. From these results, it can be seen that for 0.45 μm Millipore filters, the observed FWHM decreased from 221.7 keV for 320 μg barium to 121.3 keV for 20 μg barium carrier without any consistent trend as the carrier amount was decreased. The data showed a scattering trend for carrier amounts below 120 μg which was consistent for 0.45 μm Millipore filters. As pointed out in our previous study (Lim and Dave, 1981; Sill, 1983) factors such as the uniformity of the deposited sample thickness and the particle size of the final precipitate became dominant below that range, affecting the α-particle absorption characteristic and hance the overall resolution of the system. Sill (1983) improved the resolution to 60 keV by reducing the crystal size of the final deposited precipitate with the addition of a barium sulphate seeding suspension to the final precipitating solution, and also obtained high analytical recoveries (97%) for 100 μg Ba. Without the seeding suspension, his α resolutions of 130–270 keV for 100 μg Ba using 0.1 μm Tuffryn filters are similar to our present results for 0.45 μm

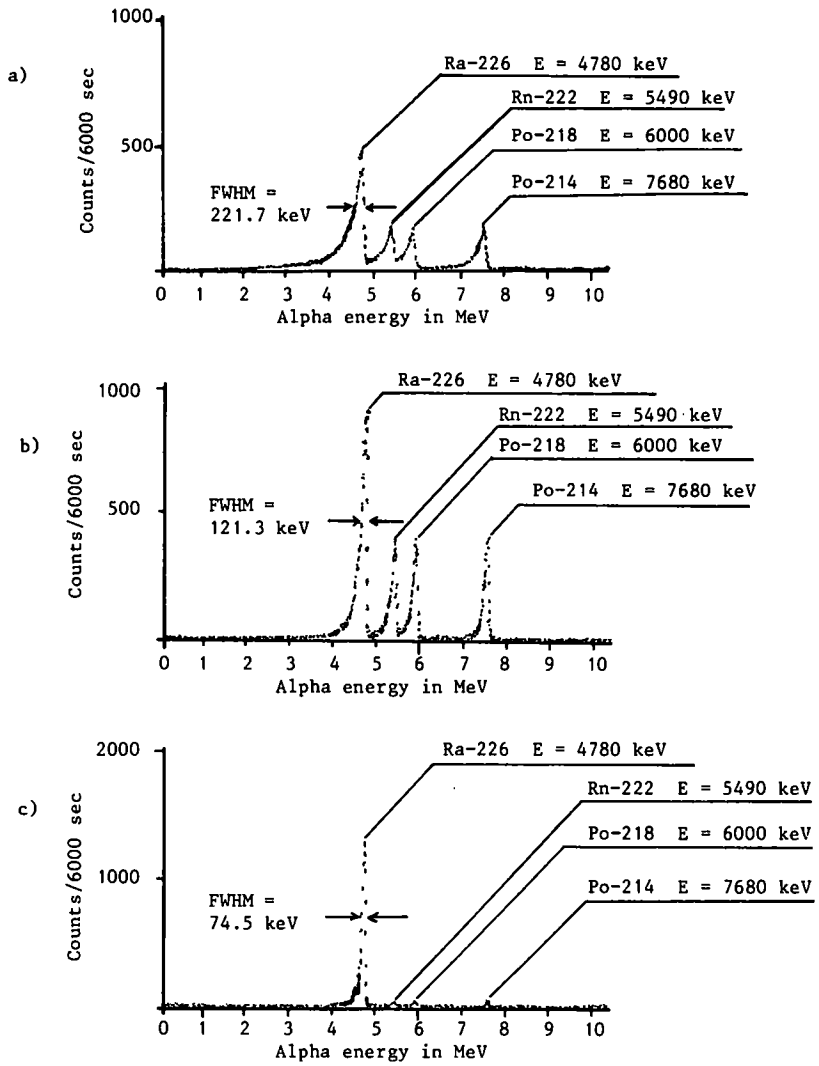

Fig. 1. ^{226}Ra α-particle energy spectra using 0.45 μm Millipore filter with barium carrier (a) 320 μg; (b) 20 μg; and (c) 0.20 μm Nucleopore polycarbonate filter with 20 μg Ba. FWHM = full width at half maximum.

Table 1. Full width half maximum (FWHM) for ^{216}Ra, 4.78 MeV peak for various amounts of barium carried added. The area of the source was 1.815 cm^2 and source detector spacing ~0.2 cm

Barium carrier added (μg)	Recovery factor ^{133}Ba (%)	Calc. barium carrier thickness (μg/cm^2) (for uniform deposition)	FWHM (keV)
Filter type: Millipore, 0.45 μm HABP 02500			
320	91.3	161.0	221.7
120	56.3	37.2	188.5
90	91.8	45.5	116.2
70	89.4	34.5	168.2
50	98.0	27.0	134.3
30	74.5	12.3	166.0
25	79.8	11.0	127.8
20	84.6	9.3	121.3
250	81.0	111.6	229*
100	67.5	37.2	229*
Filter type: Nucleopore, 0.2 μm polycarbonate			
20	67.4	7.5	74.5
20	65.6	7.2	67.0

*Data from Lim and Dave (1981).

Millipore filters as the two procedures were basically similar.

In our study, we believed the resolution could be further improved by:

(1) reducing the barium carrier concentration in the final precipitating solution to near its solubility limits, thereby decreasing the particle size of the preciptiate: and

(2) creating uniform depositional conditions by providing increased filter resistance. The latter was achieved by using 0.2 μm Nucleopore polycarbonate membrane filters which provided about three times higher resistance to liquid filtration than 0.45 μm Millipore filters, since the variation in pore size distribution of the former was less.

Figure 1(c) shows the improvement in the resolution with 20 μg Ba where the FWHM decreased from

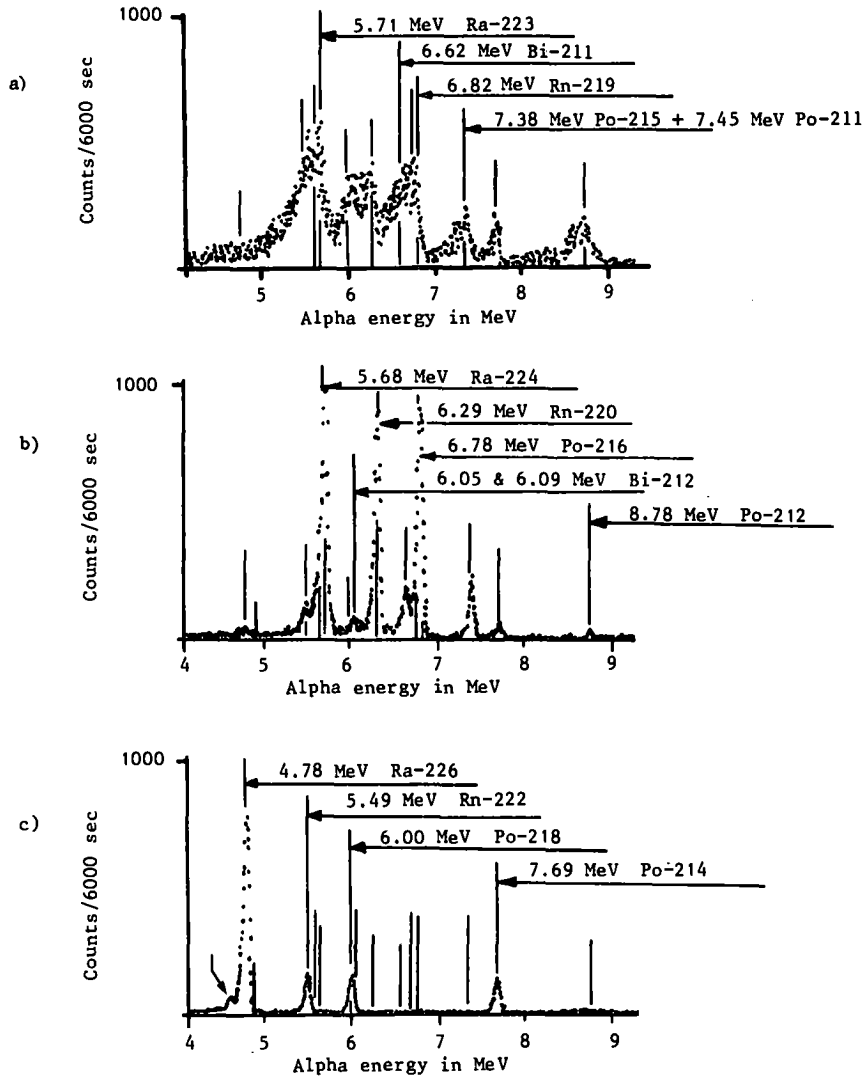

Fig. 2. Expanded α-particle energy spectra of radium isotopes (a) 0.45 μm Millipore with 320 μg Ba; (b) 0.20 μm Nucleopore with 40 μg Ba; and (c) ^{226}Ra spectrum only, 0.2 μm Nucleopore with 20 μg Ba.

121.3 keV for 0.45 μm Millipore filters to between 67 and 74.5 keV for 0.2 μm Nucleopore filters. Similar values were obtained using Sill's (1983) method. The best resolutions obtained for commercially electrodeposited mixed radionuclides, ^{239}Pu, ^{241}Am and ^{244}Cm source (Amersham), were respectively 70.3, 73.8 and 103-1 keV for 5.16 MeV ^{239}Pu, 5.49 MeV ^{241}Am and 5.81 MeV ^{244}Cm α-particle energy peaks. A resolution of 67 keV was obtained for the 5.49 MeV ^{222}Rn peak of a residual spectrum of ^{226}Ra daughters attached to the detector surface after exposing the detector to a high activity (approx 36 Bq) ^{226}Ra source for 2 h. For the present sample detector geometry, the FWHM of the residual spectrum 67.0 keV represented the best achievable resolution of the system.

It is readily seen from these results that by depositing the final precipitate on 0.2 μm Nucleopore filters, the α-resolution of the system could be considerably improved to its practical limits without much loss in the analytical recovery factors ranging between 65 and 85% (Table 1). Because of the reduced Ba amounts these values are slightly lower than those of Sill's (1983). The advantage of the present method is that it is a simplified procedure requiring less preparation time.

The effect of the high resolution obtained or uranium tailings porewater samples containing ^{223}Ra, ^{224}Ra and ^{226}Ra isotopes is clearly demonstrated in Fig. 2. For comparison purposes, Fig. 2(c) also shows a ^{226}Ra spectrum obtained with a 0.2 μm Nucleopore filter and 20 μg barium carrier. Note that the resolution of the 4.602 and 4.785 MeV, ^{226}Ra peaks is similar to that described by Sill (1983).

From Fig. 2 it is evident that although there is a clear separation of ^{226}Ra from ^{223}Ra and ^{234}Ra peaks, component resolutions among ^{222}Rn (5.490 MeV), ^{223}Ra (5.61, 5.71 and 5.75 MeV), and ^{234}Ra (5.45 and

Table 2. Equilibrium ratio between ^{226}Ra and its daughter isotopes: ^{222}Ra, ^{218}Po and ^{214}Po, at time $t = 60$ days after radium separation. Expected equilibrium ratio = 100%

Sample No.	FWHM (keV)	^{222}Rn/^{226}Rn	^{218}Po/^{222}Rn	^{214}Po/^{222}Rn	
1	221.7	106.1	77.1	84.7	
2	120.0	84.0	100.0	96.4	
3	76.0	72.0	93.1	95.9	$\bar{X} = 94.8$
4	67.0	55.0	92.7	90.8	$\sigma = 3.3$

Sample 1—^{226}Ra standard solution, precipitate deposited on 0.45 μm Millipore filter: barium carrier = 320 μg.
Sample 2—^{226}Ra standard solution, precipitate deposited on 0.22 μm Millipore filter: barium carrier = 40 μg.
Sample 3—^{226}Ra standard solution, precipitate deposited on 0.2 μm Nucleopore filter: barium carrier = 40 μg.
Sample 4—^{226}Ra standard solution, precipitate deposited on 0.2 μm Nucleopore filter: barium carrier = 20 μg.

5.68 MeV) peaks is not possible because of spectral interference. Thus, in a sample containing all three isotopes, ^{226}Ra can be measured directly, but the presence of the other two isotopes can only be inferred qualitatively. Indirect determinations of ^{223}Ra and ^{224}Ra from their daughter products ^{215}Po for ^{223}Ra, and ^{212}Po for ^{224}Ra which are clearly resolved (as shown in Fig. 2) can be accomplished after a certain ingrowth period, provided appropriate corrections are made for the loss of radon isotopes from the sample. Table 2 shows the equilibirum ratios for ^{222}Rn/^{226}Ra, ^{218}Po/^{222}Rn and ^{214}Po/^{222}Rn for ^{226}Ra isotope after an ingrowth period of 60 days.

It can be seen here that with the decrease in the barium carrier concentration, there is a significant loss of radon gas from the sample with only 55% of the equilibrium concentration retained for a sample containing 20 μg Ba carrier. The loss of radon gas is caused by the decrease in the diffusion path related to crystal size, and attenuation of the recoil radon atoms as the carrier thickness is reduced. On the other hand, the equilibrium ratio between radon and its daughter products is close to 95% for all samples with a resolution between 67 and 120 keV, and Ba carrier 20–40 μg. For samples containing a higher concentration of barium carrier (320 μg, FWHM = 221.7 keV), the calculated ratio between radon and the daughter products is less than 100% which was caused by the poor resolution of the ^{226}Ra, ^{222}Rn and ^{218}Po peaks as the spectral overlap was significant (see Fig. 1).

For a given sample, the measured retention ratio for ^{222}Rn/^{226}Ra at equilibirum can be used to correct for daughter activities in calculating ^{223}Ra and ^{224}Ra from their ingrown daughter concentrations. Alternatively, in a sample containing ^{223}Ra and ^{224}Ra isotopes, the activities can be determined as follows:

(1) At time $t = t_0$ (~ 0), immediately following the separation of radium isotopes from their parents, determine the combined activity, X, of ^{223}Ra and ^{224}Ra from their integrated decay peaks (5.45 –5.71 MeV), such that:

$$A\,C_{223}(0) + B\,C_{224}(0) = X \quad \text{at} \quad t = t_0 \qquad (1)$$

where,

A = activity fraction of ^{223}Ra at $t = t_0$: $\exp(-\lambda_1 t_0)$

B = activity fraction of ^{224}Ra at $t = t_0$: $\exp(-\lambda_1' t_0)$

$C_{223}(0)$ = activity of ^{223}Ra at $t = 0$

$C_{224}(0)$ = activity of ^{224}Ra at $t = 0$,

and λ_1, and λ_1' are decay constants for ^{223}Ra and ^{224}Ra, respectively. It is assumed in the above expression that the activity of ingrown ^{222}Rn daughters from the ^{226}Ra isotope was negligibly small for the short counting period.

(2) After a certain ingrowth period of daughters, at time $t = t_g$, determine the activity ratio of ^{215}Po/^{212}Po as:

$$(^{215}\text{Po}/^{212}\text{Po})_{t_g} = Y \qquad (2)$$

where, the activities of ^{215}Po and ^{221}Po at $t = t_g$ are given by:

$$^{215}\text{Po}\,(t_g) = D\,C_{223}(0)$$

$$^{212}\text{Po}\,(t_g) = F\,C_{224}(0) \qquad (3)$$

where, D and F are expressed in terms of decay constants as:

$$D = \frac{\lambda(^{215}\text{Po})}{\lambda(^{223}\text{Ra})}\left(\sum_{n=1}^{3} a_{3n}\exp(-\lambda_n t_g)\right) \qquad (4)$$

for ^{223}Ra series, and

$$F = \frac{\lambda'(^{212}\text{Po})}{\lambda'(^{224}\text{Ra})}\,\text{Br}\left(\sum_{n=1}^{6} a_{6n}\exp(-\lambda'_n t_g)\right) \qquad (5)$$

for ^{224}Ra series,
where Br = branching ratio (0.64) for ^{212}Bi to ^{212}Po and

$$a_{mn} = \frac{\lambda_1\lambda_2\ldots\lambda_{m-1}}{(\lambda_m-\lambda_n)(\lambda_{m-1}-\lambda_n)\ldots \ldots(\lambda_{m-r}-\lambda_n)(\lambda_2-\lambda_n)(\lambda_1-\lambda_n)} \qquad (6)$$

where, $m > n$ and $m - r \neq n$, and

$$a_{mm} = \frac{\lambda_1\lambda_2\ldots\lambda_{m-1}}{(\lambda_{m-1}-\lambda_m)(\lambda_{m-2}-\lambda_m)\ldots(\lambda_1-\lambda_m)} \qquad (7)$$

for $m = n$.
$\lambda_1, \lambda_2 \ldots \lambda_n$ = decay constants of ^{223}Ra, ^{219}Rn and

Table 3. Comparisons between ^{133}Ba and ^{226}Ra recovery factors and the observed (true) ^{226}Ra counts at 100% recovery. ^{226}Ra recovery factors were calculated using the instrumental efficiency factor $\epsilon = 0.224$, and true counts = 497.5

Sample No.	Remark	Recovery ^{133}Ba (%)	^{226}Ra (counts/6000 s)	100% ^{226}Ra (counts/6000 s)	Recovery ^{226}Ra (%)	Recovery ratio (%Ra/%Ba)
1	Std procedure	71.6	382	534	76.8	1.07
2	Std procedure	90.4	454	502	91.3	1.01
3	Std procedrue	90.4	408	451	82.0	0.91
4	Std procedure	90.5	400	442	80.4	0.89
5	Std procedure	87.8	393	447	79.0	0.90
6	Std procedure	86.8	406	468	81.6	0.94
7	Std procedure	87.0	391	450	78.6	0.90
8	Std procedure	85.0	371	436	74.6	0.88
9	Std procedure	90.0	413	459	83.0	0.92
10	Std procedure	86.7	384	443	77.2	0.89
11	Prec. at pH = 5.90*	76.2	369	484	74.2	0.97
12	Prec. at pH = 5.45	81.0	404	499	81.2	1.00
13	Prec. at pH = 4.98	92.4	420	455	84.5	0.91
14	Prec. at pH = 4.48	88.7	347	391	69.8	0.79
15	Prec. at pH = 3.95	97.6	385	395	77.4	0.79
16	Prec. at pH = 5.98	89.8	390	434	78.4	0.87
17	Prec. at pH = 5.25	87.9	389	443	78.2	0.89
18	Prec. at pH = 4.99	99.3	462	465	92.9	0.94
19	Prec. at pH = 5.30	97.5	416	427	83.7	0.86
20	Prec. at pH = 4.56	68.8	329	478	66.2	0.96
21	Prec. at pH = 4.68	24.4	98	402	19.7	0.81
22	pH = 1.18; pH = 5.5†	77.0	374	486	75.2	0.98
23	pH = 3.42; pH = 6.5	0.0	6	465	1.2	—
24	pH = 3.38; pH = 6.0	0.0	2	465	0.4	—
25	pH = 3.3; pH = 5.5	67.3	312	464	62.7	0.93
26	pH = 3.25; pH = 5.25	83.1	376	452	75.6	0.91
27	pH = 3.3; pH = 5.0	79.4	350	441	70.4	0.89
28	pH = 3.4; pH = 4.8	68.2	331	485	66.6	0.98
29	pH = 3.0; pH = 6.5	0.0	2	465	0.4	—
30	pH = 3.42; pH = 4.8	80.0	331	414	66.6	0.83
31	Final + 0.05 mg AS‡	0.0	2	465	0.4	—
32	Final + 50 mg AS‡	0.0	2	465	0.4	—
33	Final + 21 mg AS‡	0.0	1	465	0.2	—
34	Final + 125 mg AS‡	13.7	80	583	16.1	1.17
35	Final + 115 mg AS‡	72.2	373	517	75.0	1.04
36	Final + 75 mg AS‡	56.3	292	519	58.7	1.04
37	Final + 2 mg AS‡	0.0	3	465	0.6	—
38	Final + 50 mg AS‡	0.0	2	465	0.4	—
39	Final + 75 mg AS‡	67.0	341	509	68.6	1.02
40	Final + 100 mg AS‡	74.0	371	501	74.6	1.01
			Average: 464.9			0.93
			SD: 44			0.08

*Final precipitation at specified pH.
†First precipitation at pH = 1.18, and second at pH = 5.5.
‡AS—Amount of ammonium sulphate added to final precipitating solution.

^{215}Po, etc. $\lambda_1' \ldots \lambda_n'$ = decay constants of ^{224}Ra, ^{220}Rn ... ^{212}Po etc.

Solving equations (1) to (3) we have:

$$C_{223}(0) = \frac{XYF}{(AYF + BD)} \tag{8}$$

and

$$C_{224}(0) = \frac{XD}{(AYF + BD)}. \tag{9}$$

Thus, the concentrations of ^{223}Ra and ^{224}Ra can be obtained by measuring parameters X and Y with A, B, D and F known.

It was assumed in the above derivations that there was no significant difference in the retention characteristics of various radon isotopes and their daughter products for the three radium isotopes. Use of computerized models such as those developed by Wätzig and Westmeier, (1978), Westmeier (1984), and Williams (1984) for complex α-particle spectra could further the analytical capabilities of the present high resolution technique.

Barium–Radium Recovery

Table 3 gives the calculated recovery factors for ^{133}Ba and ^{226}Ra and the true and corrected ^{226}Ra counts at 100% recovery for 6000 s. The recovery factors for ^{226}Ra were calculated using the measured value of the instrumental efficiency factor, $\epsilon = 0.224$ and source disintegration per minute (dpm) = 22.2, equivalent to total counts/6000 s = 497. The observed frequency distributions for ^{133}Ba and ^{226}Ra recovery factors are plotted in Fig. 3. Figure 4 shows the correlation between the observed ^{226}Ra counts and ^{133}Ba recovery factors with a linear relationship of the form:

$$Y\ (^{226}\text{Ra counts/6000 s}) = 4.57 \cdot (\%\ ^{133}\text{Ba recovery})$$

with the coefficient of regression $r^2 = 0.98$ and standard deviation of the slope = 0.05.

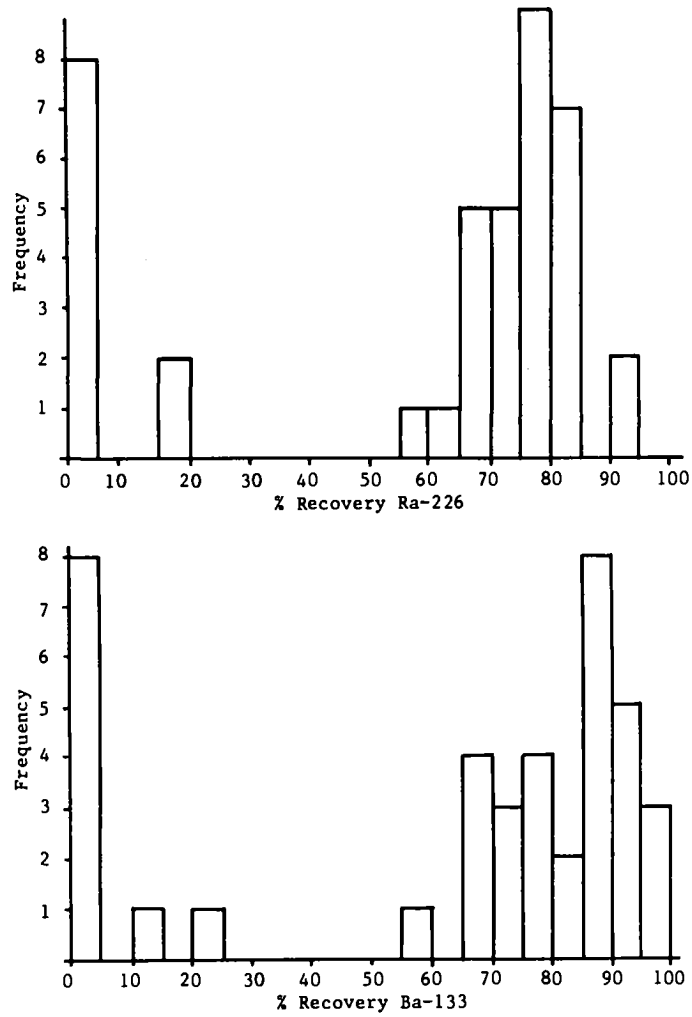

Fig. 3. Frequency distribution of ^{133}Ba and ^{226}Ra recovery factors.

Also shown in Table 3 and Fig. 4 are the observed and calculated ^{226}Ra counts at 100% recovery (curve "D"). Note that the average ^{226}Ra counts calculated for 100% recovery were 465 ± 44 compared to the expected value of 497, the difference being of no statistical significance ($P > 0.05$). Figure 5 shows the correlation between the two calculated recovery factors for ^{226}Ra and ^{133}Ba. The average value of the ^{226}Ra/^{133}Ba recovery ratio was calculated as 0.93 ± 0.08 compared to the expected value of 1.0. In the final $BaSO_4$ precipitation procedure, it was aimed at varying the overall recovery of Ba and Ra sulphates over a wide range by adjusting the controlling parameters such as pH and sulphate concentrations, but the final recovery was always high (>60%), except for eight samples where it was zero and for two samples where it varied from 10 to 30%. No attempt was made to vary the barium carrier concentration to obtain different recovery factors, and in the routine analytical procedure the carrier concentration was always constant. As seen from the data, no systematic trends between low and high recoveries were identifiable.

It can thus be stated from present results that by using a chemically different isotope as a tracer (^{133}Ba) to measure chemical yield of Ra isotopes, the correlation between the two can only be expressed within a statistical uncertainty of approximately 8%. As Sill (1983) has pointed out, better correlation between these two atoms which differ in ionic radii and chemical characteristics cannot be expected to the same degree as in similar isotopic tracers. For ^{226}Ra analysis, however, there are no other radium isotopes with reasonable half-lives that can be used as tracers.

Conclusions

This study has clearly demonstrated that the α-particle resolution of the system can be improved by a factor of 3 by decreasing the barium carrier concentration to 20 μg and using a 0.2 μm Nucleopore membrane filter, without much loss in chemical recovery. The overall effect was to reduce the broadening of the α-spectral peaks because of self-absorption of α-particles within the deposited barium

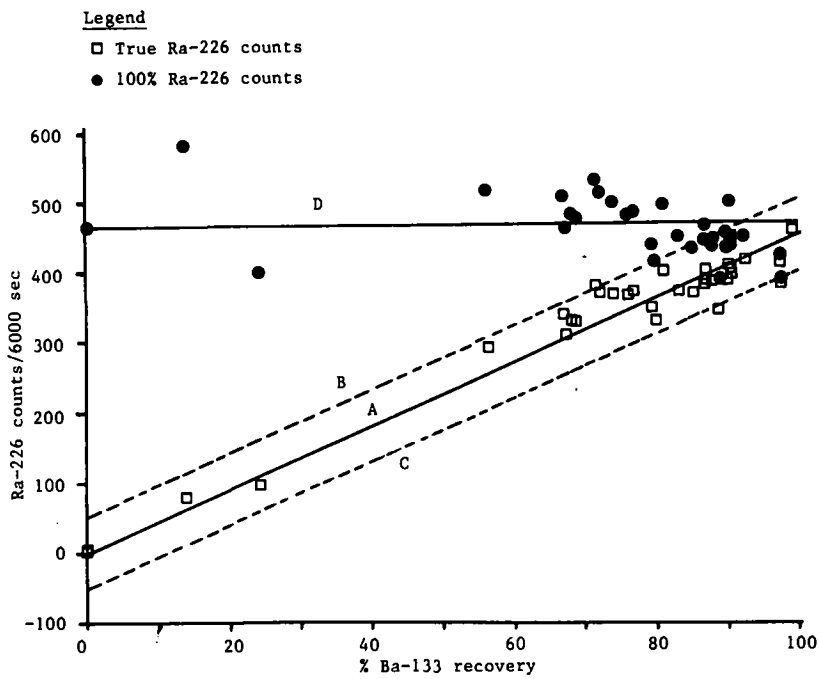

Fig. 4. Correlation between the observed ^{226}Ra counts and ^{133}Ba recovery factor curve (A) and with 95% confidence limits (curves B and C). Curve D is the calculated ^{226}Ra counts at 100% efficiency.

sulphate and its crystalline matrix. There was also a significant decrease in the retention of radon and its daughters with the decrease of barium carrier.

Correlation between ^{133}Ba and ^{226}Ra isotopic recovery factors showed that for the main Ba–Ra sulphate precipitates, the recovery factors between these two chemically different atoms can only be expressed within a statistical uncertainty of +8%.

References

Lim T. P. and Dave N. K. (1981) A rapid method of ^{226}Ra analysis in water samples using an alpha-spectroscopic technique. *CIM Bull.* **74**, 97.

Sill C. W. (1983) Determination of radium-226 by high resolution alpha-spectrometry. Report DE83-014 959. EG & G Inc., Idaho Falls, Idaho, U.S.A.

Wätzig W. and Westmeier W. (1978) Alfun—a program for the evaluation of complex alpha-spectra. *Nucl. Instrum. Methods* **153**, 517.

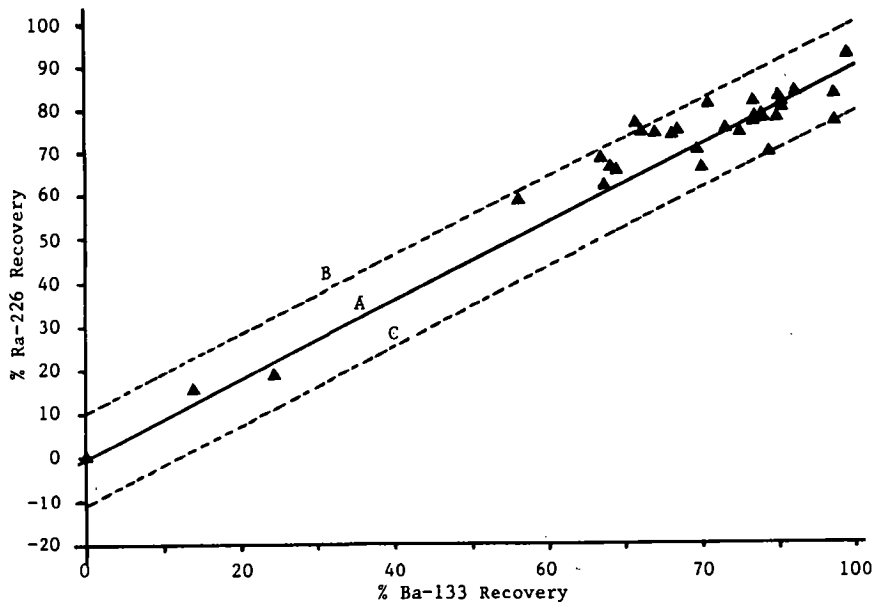

Fig. 5. Correlation between actual ^{226}Ra and ^{133}Ba recovery factors (curve A), 95% confidence limits (curves B and C).

Westmeier W. (1984) Computerized analysis of alpha-particle spectra. *Int. J. Appl. Radiat. Isot.* **35**, 263–270.

Williams R. L. (1984) A computerized alpha-particle-spectrometry system for the analysis of low-level thorium, uranium, plutonium and americium fractions. *Int. J. Appl. Radiat. Isot.* **35**, 271–277.

Zimmerman J. B. and Armstrong V. C. (1971) The determination of ^{226}Ra in uranium ores and mill products by alpha-energy spectra. *Division Report* MRP/MRL 76-11. CANMET, Energy, Mines and Resources, Canada.